ELSEVIER

Biochimica et Biophysica Acta 1231 (1995) 76–88

BBA Biochimica et Biophysica Acta

Electron transfer reactions in Photosystem II core complexes from *Synechococcus* at low temperature – difference spectrum of $P680^+ Q_A^-/P680 Q_A$ at 77 K

Bettina Hillmann, Eberhard Schlodder *

Max-Volmer-Institut für Biophysikalische und Physikalische Chemie, Technische Universität Berlin, Strasse des 17. Juni 135, D-10623 Berlin, Germany

Received 23 December 1994; revised 3 April 1995; accepted 20 April 1995

Abstract

Absorbance difference spectroscopy has been used to study electron transfer reactions at low temperature in isolated Photosystem II complexes from *Synechococcus*, when the first quinone acceptor is in the oxidized form. (1) The flash-induced absorbance difference spectrum attributed to the formation of $P680^+Q_A^-$ has been measured at 77 K between 300 nm and 900 nm. The $P680^+Q_A^-/P680Q_A$ difference spectrum in the Q_y region exhibits a marked temperature dependence. At 77 K the spectrum includes the main bleaching band at 675 nm, an absorbance increase at 681 nm, a smaller bleaching at 686 nm and a positive band at around 667 nm. The width of the main bleaching band is only ≈ 6 nm compared to about 15 nm of the 680 nm band at room temperature. It is proposed that a strong electrochromic red shift of an absorption band dominates the shape of the spectrum giving rise to an absorbance decrease at 675 nm and an absorbance increase at 681 nm. (2) While multiphasic decay kinetics of the secondary radical pair, $P680^+Q_A^-$, are found at room temperature, the decay becomes close to mono-exponential with an apparent half-life of 3 ms below 200 K. However, with a signal to noise ratio ≥ 50, two components with half-lives of ≈ 1.8 and ≈ 5 ms could clearly be resolved at 77 K. This biphasicity is attributed to frozen conformational states with a slightly different distance between P680 and Q_A. (3) In agreement with earlier work in the literature performed with PS II preparations of higher plants, we identified in PS II of *Synechococcus* three secondary donors oxidized with low quantum yield at 77 K: Cyt *b*-559, a carotenoid and a chlorophyll *a* characterized by a bleaching at 667 nm. Between 650 and 700 nm the light-induced absorbance difference spectra due to the oxidition of the secondary donor(s) and the reduction of Q_A exhibit also strong electrochromic band shifts. Predominant is a red-shift of an absorption band similar to that proposed to be present in the $P680^+Q_A^-/P680Q_A$ difference spectrum. (4) On the basis of kinetic data, regarding all three secondary donors, we conclude that Car and Cyt *b*-559 donate electrons to $P680^+$ in parallel pathways. As the rise of Car^+ formation is faster than the decay of $P680^+Q_A^-$, it is proposed that Car^+ is rapidly rereduced by Chl down to an equilibrium level.

Keywords: Photosystem II; P680; Electron transfer; Absorbance difference spectroscopy; Low temperature

1. Introduction

In Photosystem II (PS II) the sequence of light-driven electron transfer reactions leads to the oxidation of water and the reduction of plastoquinone (for reviews see Refs. [1,2]). After absorption of light by an antenna pigment, the excitation energy is transferred to a special chlorophyll *a* molecule, named P680, the primary electron donor of PS II. From the lowest excited singlet state of P680 the primary charge separation between P680 and a pheophytin *a* molecule takes place. The charge separation is stabilized by the secondary electron transfer from the reduced pheophytin to a special plastoquinone, Q_A. On the donor side, $P680^+$, a very strong oxidant capable of oxidizing water to O_2, is reduced primarily in the nanosecond time range by the donor Tyr_Z. This is a tyrosine residue of the D1-polypeptide, one of the reaction center core proteins. The oxidized Tyr_Z is in turn reduced by the oxygen-evolving complex. After irreversible inhibition of O_2 evolution, $P680^+$ is still reduced by Tyr_Z, but the electron donation is retarded by a factor of about 1000 and Tyr_Z^+ remains oxidized if no artificial electron donor is present. If Tyr_Z is

Abbreviations: Car, carotenoid; Chl, chlorophyll; Cyt *b*-559, cytochrome *b*-559; *d*, optical path for the measuring light; fwhm, full width at half maximum; Mes, 2-(*N*-morpholino)ethanesulfonic acid; PS II, Photosystem II; P680, primary electron donor of PS II; Q_A and Q_B, first and second plastoquinone electron acceptor; Tyr_Z, tyrosine residue, electron donor to $P680^+$.

* Corresponding author. Fax: +49 30 31421122.

SSDI 0005-2728(95)00068-2

still oxidized and a charge separation between P680 and Q_A occurs, $P680^+$ Q_A^- decays by charge recombination.

At low temperatures ($T \leq 100$ K), electron transfer from Q_A^- to Q_B and from Tyr_Z to $P680^+$ is blocked and half-lives between 2 and 5 ms have been reported for the charge recombination of $P680^+Q_A^-$ [3–5]. The initial signal amplitude attributed to the formation of $P680^+Q_A^-$ decreases progressively with successive flashes. This decrease was attributed to competitive electron donation to $P680^+$ by Cyt *b*-559 [6] or, when Cyt *b*-559 is oxidized prior to freezing, by another donor, presumably a chlorophyll *a* [7] or a carotenoid molecule [8], leading to long-lived charge separated states. The pathways and kinetics of electron donation to P680 at low temperature are not well understood and different models have been proposed [4,7,9].

At room temperature the charge recombination kinetics of the secondary radical pair, $P680^+Q_A^-$, were found to deviate significantly from a single exponential relaxation, in contrast to what is expected for unimolecular reactions. Using PS II complexes from *Synechococcus*, at least three exponentials were required for a satisfactory fit of the time-course [10]. It has been proposed that the complex kinetics can be attributed to three different (or a distribution of) conformational states of the PS II reaction center and that the transition between these states is slow compared with the time-scale of charge recombination [11]. Evidence that conformational substates in proteins may be the origin of non-exponential relaxation comes from studies of a variety of systems [12–16]. The assumption that structural heterogeneities lead to a distribution of activation enthalpies for the charge recombination of $P680^+Q_A^-$ and/or to a distribution of the $P680^+Q_A^-$ electron transfer distance can explain the non-exponential decay of $P680^+Q_A^-$. In this work we look for deviations from a mono-exponential decay kinetics at low temperatures. For our investigation we used isolated O_2-evolving PS II core complexes from *Synechococcus* [17]. Compared to chloroplasts or PS-II-enriched membrane fragments from higher plants used for the most part in previous work, PS II core complexes have less chlorophylls per reaction center and are optically clear, allowing a better signal-to-noise ratio.

The formation of the secondary radical pair is well characterized by its absorbance difference spectrum [18,19,10]. The absorbance changes in the red wavelength region have been attributed to the oxidation of P680. At room temperature the difference spectrum in the red is dominated by the bleaching of the Q_y band of P680 and is similar to the in vitro spectrum of Chl a^+/Chl *a* [20–22] except for a red shift of the Q_y band that may be due to interactions of the pigment with the surrounding protein. Additionally, a small electrochromic bandshift at 685 nm has been observed upon reduction of Q_A [23]. Low-temperature spectra of $P680^+Q_A^-/P680Q_A$ reported so far resemble closely the room-temperature spectrum [24,25]. On the other hand, the $^3P680/P680$ spectrum shows a pronounced temperature dependence [26–28]. As the temperature is lowered, the spectral width of the Q_y-bleaching band of the $^3P680/P680$ spectrum decreases by more than a factor of 2. This is accompanied by a corresponding increase of the peak amplitude. Therefore, we reexamined the $P680^+Q_A^-/P680Q_A$ spectrum at 77 K with high spectral resolution and measured a complete spectrum between 300 nm and 900 nm that was not available until now. The low temperature $^3P680/P680$ spectrum exhibits, additionally, small bands on the short-wavelength side of the Q_y band, indicating weak excitonic coupling with neighboring pigment(s). It has been extensively studied using D1/D2/Cyt *b*-559-reaction center complexes (for recent reviews see Refs. [29,30]) to clarify the spectral features in the Q_y region and derive structural information about the primary donor in PS II. At present, the structural organization of the primary donor of PS II is still under debate. On one hand, a dimeric structure is expected based on amino acid sequence homology between the D1 and D2 in PS II and the L and M subunits of bacterial reaction center [31]; on the other hand the spectroscopic data are more in common with a monomeric nature of P680. The small exciton splitting in the Q_y region, the orientation of the triplet *z*-axis and the small Stark effect differ widely from data expected of a special pair of two Chl *a* molecules, with a structure the same as the special pair in bacterial reaction centers (for reviews see Refs. [29,30,32,33]). Another crucial point is the high redox potential of $P680^+/P680$ of > 1V, which fits better to monomeric Chl *a* in vitro [21]. Complementary information on the spectral properties of P680 can be obtained from the low temperature $P680^+Q_A^-/P680Q_A$ spectrum presented in this work.

Parts of this work were presented at the Biophysiktagung, Osnabrück, September 28–30, 1992.

2. Materials and methods

O_2-evolving PS II core complexes were prepared from the cyanobacterium *Synechococcus elongatus naegli* according to Schatz and Witt [34] and further purified by sucrose density centrifugation [35]. Tris-treated PS II complexes were obtained as described in Ref. [17]. The preparations were stored at −80°C in 20 mM Mes/NaOH (pH 6.5), 10 mM $MgCl_2$, 20 mM $CaCl_2$, about 1 M sucrose and 0–0.06% (w/w) sulfobetaine 12. The PS II preparations had a PS II/PS I ratio of more than 50, a Chl *a*/P680 ratio of about 50 and an O_2 flash yield of about 1 O_2 per 350 Chls per flash. For further characterization of the PS II core complexes see Ref. [17].

Before measurements, a PS II preparation was thawed and diluted with MMCM (20 mM Mes/NaOH (pH 6.5), 10 mM $MgCl_2$, 20 mM $CaCl_2$ and 0.5 M mannitol) to adjust the chlorophyll concentration and with glycerol as cryoprotectant to give a final glycerol concentration of about 60% (v/v). If redox reagents (about 3 mM ferri-

cyanide or 3 mM ascorbate plus 2 mM hydroquinone) had been added, the sample was incubated at room temperature for about 15 min before freezing in a variable temperature liquid nitrogen cryostat (Model DN 1704 from Oxford Instruments).

The spectrum of the absorbance changes between 300 and 720 nm were measured with an apparatus as described in Ref. [10]. The bandwidth of the monochromator (Bausch and Lomb) was 5 nm and reduced to 1 nm in the Q_y region to increase the spectral resolution. For measurements in the red wavelength region the photomultiplier was placed about 1 m behind the cuvette in order to reduce the fluorescence collected by the photomultiplier. A similar set-up was used for measurements in the wavelength region between 700 and 1000 nm except that the measuring wavelength was selected by Schott interference filters placed before the sample and in front of the silicon photodiode detector (OSD 100-5T, Centronic) that was coupled to an amplifier (TEK AM 502, Tektronix).

Absorbance changes at 676 nm were additionally measured using a laserdiode (TOLD 9200, Toshiba) as a measuring light source. With a microscope lens and a converging lens, the laser beam was focused on the active area of a silicon photodiode placed about 1.5 m behind the cryostat. The diameter of the beam at the sample was about 1 cm. The measuring light was pulsed by a photoshutter (pulse duration: 60 ms) to reduce excitation of the sample. This set-up minimized very efficiently the flash-induced fluorescence artefact and allowed measurements with nanosecond time resolution. For measurements in the nanosecond range, the detection system (photodiode-preamplifier module: C30952A, RCA; amplifier: 461A, Hewlett Packard; transient recorder: Biomation 6500, Gould; signal averager: Nicolet 1170) had an electrical bandwidth of 1 kHz to 50 MHz. In the micro- and millisecond range a photodiode (SGD 444, EG and G) with a variable load resistance coupled to a TEK AM 502 amplifier by Tektronix has been used. Absorbance changes at 824 nm were mostly measured with the apparatus described previously [36].

Low-temperature absorbance spectra and absorbance difference spectra induced by continuous light (white light, approx. 50 mW/cm^2 in the wavelength region from 350 nm to 700 nm) were measured with a spectral resolution of 1 nm using different spectrophotometers (Shimadzu UV-3000 or Cary 5 from Varian).

3. Results

3.1. Kinetics of the charge recombination between $P680^+$ and Q_A^- at 77 K

Fig. 1 shows the time-course of flash-induced absorbance changes at 676 nm and at 824 nm observed in PS II core complexes from *Synechococcus* at 77 K. The

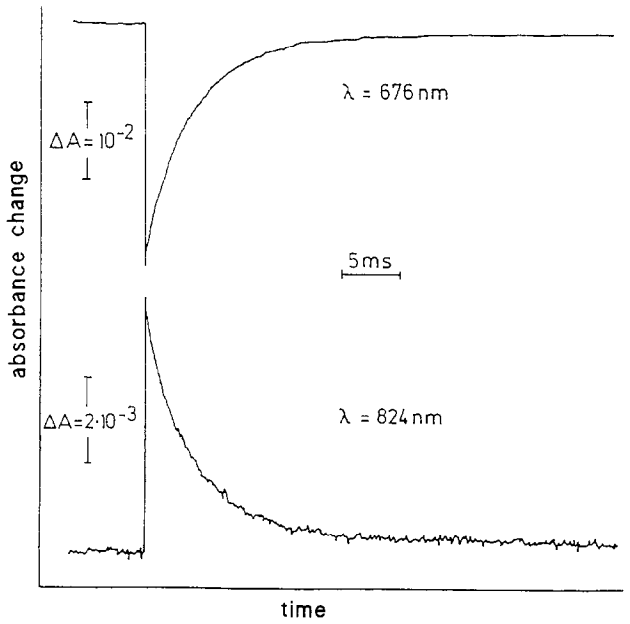

Fig. 1. Time-course of the flash-induced absorbance changes in PS II core complexes from *Synechococcus* at 77 K measured at 676 nm (20 μM Chl; 3 mM $K_3[Fe(CN)_6]$; $d = 0.36$ cm; average of the first 8 transients) and at 824 nm (40 μM Chl; 2 mM $K_3[Fe(CN)_6]$; $d = 1$ cm; average of the first 4 transients). Excitation by saturating laser flashes at 532 nm (fwhm, approx. 3 ns).

signals are the average of the first few flashes. To prevent the accumulation of the state Cyt *b*-559$^+$P680PheoQ$_A^-$ that is irreversibly formed with low quantum yield by electron donation of Cyt *b*-559 to $P680^+$ [4], Cyt *b*-559 was chemically oxidized by incubation of the sample with ferricyanide in the dark before freezing. The transient absorbance changes are attributed to the formation and subsequent decay of $P680^+Q_A^-$ as can be judged from the absorbance difference spectrum (see Fig. 3 and Fig. 4) and the decay kinetics. The time-course of the absorbance changes is close to a mono-exponential decay. Fitting the decay with a single exponential (plus a constant) yielded a half-life of (3 ± 0.5) ms, in agreement with earlier studies of the charge recombination of $P680^+Q_A^-$ in PS II of higher plants [3–5,37]. Variations due to different preparations are included in the margin of error. However, the quality of these fits is not satisfactory for signals with high signal-to-noise ratio. The residuals indicate significant deviations of the recombination kinetics from a single exponential process. Fig. 2 shows the time-course of the absorbance change at 826 nm in the 80 ms time range (upper trace) and the differences between the observed signal and the calculated curves obtained by fitting the time-course of the absorbance change to a single exponential decay plus a constant (middle trace) or to a double exponential decay plus a constant (lower trace). The constant accounts for the small absorbance change which is not decaying in the time window of the measurement. This non- or slowly reversible phase may be assigned to stable charge separated

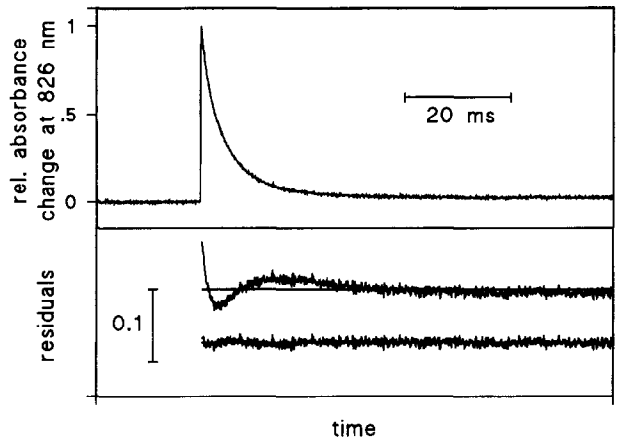

Fig. 2. Time-course of the flash-induced absorbance changes in PS II core complexes from *Synechococcus* at 77 K measured at 826 nm (top) and the differences between the observed signal and the calculated curves obtained by fitting the time-course of the absorbance change to a single exponential decay plus a constant (middle) or to a double exponential decay plus a constant (bottom). The constant accounts for the small absorbance change not decaying in the time window of the measurement. The best fits yielded the following half-lives and relative amplitudes: middle: $t_{1/2} = 3.4$ ms (96.6%) and 3.4% for the constant; bottom: $t_{1/2} = 1.8$ ms (53.2%) and $t_{1/2} = 5.1$ ms (44.2%) for the two exponential phases and 2.6% for the constant.

states formed by electron donation of secondary donors (Chl and Car) to $P680^+$ with low yield in competition to charge recombination (see below). As seen in Fig. 2, the residuals calculated for the single exponential fit (middle trace) show non-random deviations from zero well above the noise level, whereas the deviations are fairly random for the double exponential fit with the following fit parameter: $t_{1/2} = 1.8$ ms (53.2%) and $t_{1/2} = 5.1$ ms (44.2%) for the two exponential phases and 2.6% for the constant. A satisfactory fit of the decay curve measured at 676 nm was obtained with nearly the same values for the half-lives and relative amplitudes ($t_{1/2} = 1.7$ ms (54.5%) and $t_{1/2} = 4.7$ ms (45.1%) for the two exponential phases and 0.4% for the constant) giving further evidence that the charge recombination of $P680^+Q_A^-$ deviates from a single exponential process. It should be noted that a signal-to-noise ratio of better than about 50 is necessary to resolve two exponential phases, explaining why the biphasicity at low temperature was not recognized in previous studies.

The time-course of flash-induced absorbance changes at 824 nm has been measured as a function of temperature (not shown). Between 77 K and about 200 K the decay kinetics are nearly temperature-independent as observed with spinach chloroplasts [38]. Above 200 K the rate of charge recombination increases with increasing temperature indicating a thermally activated process. At room temperature the recombination kinetics become strikingly multiphasic. The predominant decay phase has a half-life of about 170 μs, whereas the half-life of the slowest decay component is about 5 ms. A satisfactory fit of the time-course requires at least three exponentials with half-lives and relative amplitudes similar to those reported in our previous study using PS II core complexes from *Synechococcus* [10].

3.2. $P680^+Q_A^-/P680Q_A$ absorbance difference spectrum

In order to get the absorbance difference spectrum associated with the formation of the secondary radical pair, the amplitude of the flash-induced absorbance changes has been measured as function of the wavelength. Fig. 3 shows the spectrum between 300 nm and 650 nm. In this wavelength region the low temperature difference spectrum resembles that measured at room temperature [10,19]. It is characterized by (a) an absorption increase at 320 nm indicating the reduction of Q_A, (b) a strong bleaching at 433 nm and a broad absorption decrease around 630 nm due to the oxidation of P680 and (c) a bandshift (C-550) centered at 543 nm that is caused by the electric field of

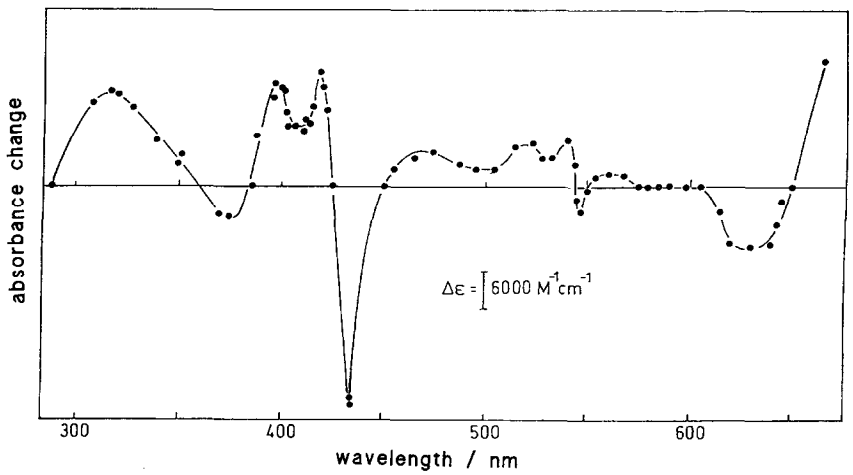

Fig. 3. Spectrum of the flash-induced absorbance changes in the wavelength region between 300 nm and 650 nm measured in PS II core complexes at 77 K in the presence of 3 mM $K_3[Fe(CN)_6]$ attributed to the formation of the secondary radical pair, $P680^+Q_A^-$.

Q_A^-. Compared to the room-temperature spectrum, the 77 K spectrum exhibits the following differences. The amplitude of the C-550 bandshift is larger, an additional small absorption band around 520 nm is observed and the trough at 408 nm is more pronounced. These differences may result from stronger electrochromic effects at low temperature caused by the electric fields of $P680^+$ and Q_A^-. Larger absorbance changes due to electrochromic bandshifts at low temperature can be explained for the most part by the sharpening of absorption bands with decreasing temperature.

Fig. 4 shows the $P680^+Q_A^-/P680Q_A$ difference spectrum between 660 nm and 710 nm at 77 K (solid line) and at 298 K (dashed line). The difference spectrum in the near infrared between 700 nm and 900 nm at 77 K is shown in the inset of Fig. 4. The near infrared spectrum is in good agreement with that reported by Mathis and Setif [39] for the formation of $P680^+$. In the Q_y region the difference spectrum at 77 K (Fig. 4, solid line) is dominated by a strong bleaching at 675 nm. Furthermore, it exhibits a smaller bleaching at 686 nm, a positive peak at about 681 and a broad absorbance increase around 666 nm. The full width at half maximum of the main bleaching band is about 6 nm. A differential molar extinction coefficient of about 230000 M^{-1} cm^{-1} for the reaction $P680Q_A \rightarrow P680^+Q_A^-$ is calculated from the absorbance change at 675 nm induced by saturating flashes using a ratio of 50 Chls per P680. At saturating excitation, the area under the curve between 650 and 695 nm corresponds to a loss of dipole strength of approx. 17 D^2 in the Q_y region. Assuming a dipole strength of 23 D^2 for the Q_y band of a Chl *a* molecule [40] and taking into account that Chl a^+ contributes in this region with a dipole strength of about 6 D^2 [22], the bleached area of 17 D^2 agrees well with the value expected for the oxidation of one Chl *a* molecule.

The accuracy of the differential molar extinction coefficients given in Fig. 3 and Fig. 4 is limited by the following: (a) A decrease of the signal amplitude was observed upon repeated measurements (see below). Therefore the difference spectra had to be corrected for signal loss. (b) Because of the sample contraction and the contraction of the plexiglas cuvette the concentration and the optical path length are not exactly known. (c) The cuvette in the cryostat was positioned at 45° to the mutually perpendicular exciting and measuring beam in most measurements. Deviations from the 45° position also cause an error regarding the optical path length. In summary, the margin of error is estimated to be about ±20%.

The difference spectrum measured at 77 K in the red wavelength region (Fig. 4, solid line) is strikingly different from $P680^+Q_A^-/P680Q_A$ spectra reported so far in the literature, which have been measured either at low temperature [24,25] or at room temperature [18,19,41]. Therefore, we repeated the measurement of the room-temperature spectrum under otherwise identical experimental conditions using Tris-treated PS II complexes from *Synechococcus*. In order to prevent rereduction of $P680^+$ by Tyr_Z, the immediate electron donor to $P680^+$, Tyr_Z was oxidized by a preflash given 80 ms prior to the laser flash. Under these conditions charge recombination is observed in nearly all PS II complexes. The $P680^+Q_A^-/P680Q_A$ spectrum obtained in this way (Fig. 4, dashed line) is very similar to room-temperature spectra reported earlier [18,19]. Moreover, the low-temperature $P680^+Q_A^-/P680Q_A$ difference

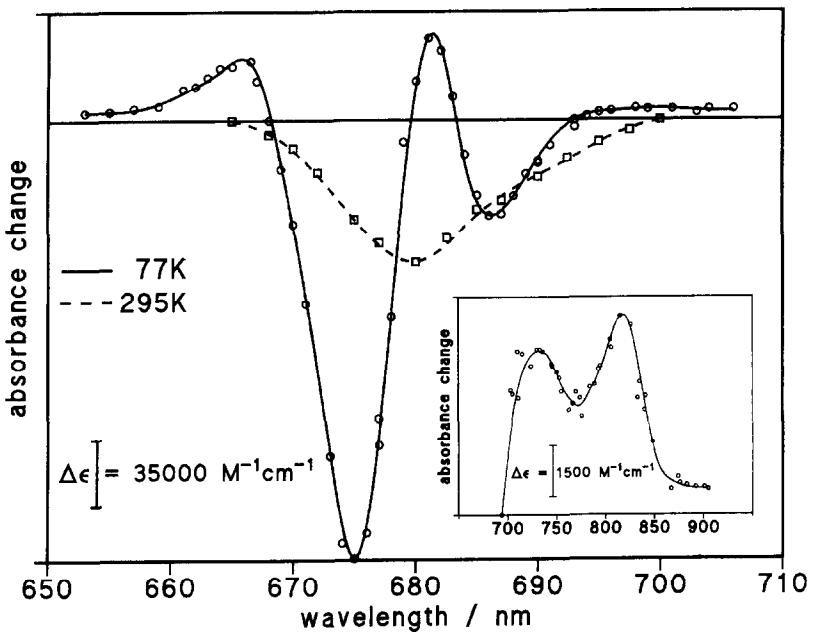

Fig. 4. Difference spectrum of $P680^+Q_A^-/P680Q_A$ at 77 K (solid line) and at room temperature (dashed line) in the 650 – 710 nm range. Inset: Difference spectrum of $P680^+Q_A^-/P680Q_A$ at 77 K in the near infrared between 700 and 900 nm. See text for further details.

spectrum in the Q_y region described above for PS II complexes from *Synechococcus* has been confirmed using PS-II-enriched membrane fragments from spinach [42].

In an attempt to explain the position of the main bleaching band in the Q_y region found at low temperature (675 nm, instead of 680 nm), it may be proposed that $P680^+$ initially formed by the flash is reduced by another Chl molecule with an absorption maximum around 675 nm in the time range of nano- to microseconds and that the 3 ms decay reflects the charge recombination between Chl^+ and Q_A^-. This electron transfer might be prevented at room temperature due to the fast rereduction of $P680^+$ by Tyr_Z. Therefore, we performed measurements at low temperature with nanosecond time resolution at 676 nm and 824 nm (not shown). No evidence for such electron transfer was obtained from the kinetic analysis of the absorbance changes at either wavelength, and the amplitude taken at about 10 ns (the instrument-limited rise time was about 7 ns) coincided with the initial amplitude of the millisecond decay phases.

3.3. Competition between charge recombination and electron donation to $P680^+$ by secondary donors

When Cyt *b*-559 was reduced, which was achieved by addition of ascorbate and hydroquinone prior to freezing, the kinetics and the difference spectrum of the flash-induced absorption changes are virtually the same as described above for samples with Cyt *b*-559 in the oxidized state. In both cases, a progressive decrease of the initial flash-induced absorbance changes was observed with increasing flash number. This decrease can be explained by an electron transfer from secondary donors to $P680^+$ that occurs with low quantum yield in competition to the recombination of $P680^+Q_A^-$. The stable or at least long-lived state, characterized by the oxidized secondary donor and reduced Q_A, accumulates progressively with increasing flash number or during continuous illumination.

In accordance with earlier work in the literature using PS II of higher plants [3,4,6–8,43], we observed the photooxidation of three distinct secondary donors at 77 K by light-minus-dark absorbance difference spectra: a carotenoid (Car), a chlorophyll (Chl) and Cyt *b*-559. The spectra were obtained by continuous illumination of PS II complexes from *Synechococcus* at 77 K under different redox conditions. Fig. 5 shows the light-minus-dark absorbance difference spectra measured in the presence of oxidized Cyt *b*-559. The absorbance spectrum before illumination at 77 K was subtracted from that measured after 5 min illumination and subsequent dark adaptation for about 2 min (a,b,c) or 80 min (d,e,f). The bandshift (C-550) giving rise to the absorbance increase at 540 nm and the absorbance decrease at 546 nm (Fig. 5 a,d) is associated with the reduction of Q_A. In the red wavelength region (Fig. 5 b,e) the absorbance changes are attributed to the bleaching of an absorption band at 667 nm and to band

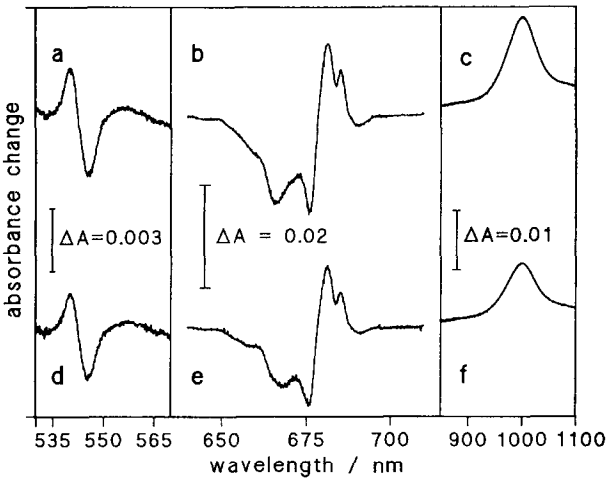

Fig. 5. Light-minus-dark absorbance difference spectrum induced by continuous illumination of PS II core complexes from *Synechococcus* at 77 K. 3 mM $K_3[Fe(CN)_6]$ was added before freezing in order to oxidize Cyt *b*-559. The absorbance spectrum before illumination at 77 K was subtracted from that measured after 5 min illumination (white light with approx. 50 mW/cm^2) and subsequent dark adaptation for about 2 min (a,b,c) or 80 min (d,e,f). The absorbance changes are normalized to 20 μM Chl and $d = 1$ cm. c,d: spectral resolution: 3 nm, scan speed: 1.5 nm/s, scan range: 1100–750 nm; a,b,d,e: spectral resolution: 1 nm, scan speed: 0.75 nm/s, scan range: 750–450 nm.

shifts of neighboring pigments (chlorophyll and/or pheophytin molecules) induced by the electric field of the oxidized donor and Q_A^-. The bleaching suggests that a chlorophyll *a* absorbing at 667 nm is oxidized. Presumably this Chl acts as secondary donor and the state $Chl^+P680Q_A^-$ accumulates during continuous illumination. The predominant band shift is the red shift of an absorbance band giving rise to the absorbance decrease at 676 nm and the absorbance increase at 681 nm. The peaks at 685 nm (positive) and 690 nm (negative) are possibly related to a blue shift of an absorption band around 687 nm. A similar bandshift near 686 nm has been observed at room temperature on the reduction of Q_A [23]. In the near-infrared region (Fig. 5, c,f) a broad absorbance band appears around 1000 nm with a full width at half maximum of about 70 nm. This band is characteristic of the carotenoid radical cation [8,44], indicating that also the state $Car^+P680Q_A^-$ is formed by continuous illumination. The comparison between the upper and lower curves in Fig. 5 indicates that the light-induced absorbance changes decay at least partly in the dark after illumination. Note that the C550 signal was measured in one scan from 750 nm to 500 nm, i.e., it was recorded at about 6 min after illumination. Therefore, the signal amplitude of Fig. 5a has already decreased more than the signals depicted in Fig. 5b and 5c. The yield of oxidized secondary donors can be roughly estimated using an extinction coefficient for the carotenoid radical cation of 10^5 M^{-1} cm^{-1} at 1000 nm [44] and a differential extinction coefficient of $9 \cdot 10^4$ M^{-1} cm^{-1} for the oxidation of chlorophyll *a* at the maximum

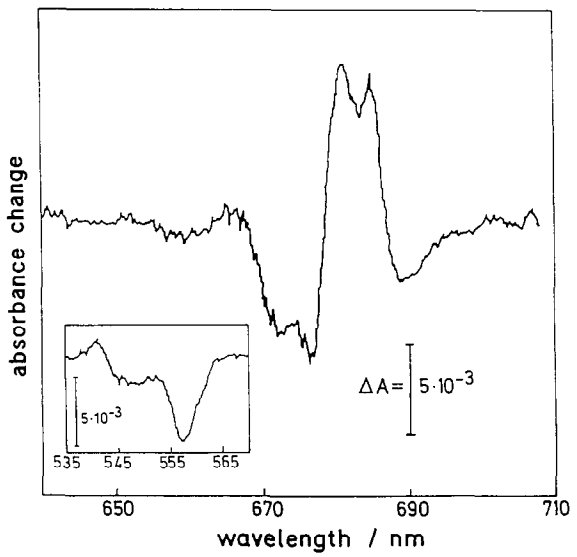

Fig. 6. Light-minus-dark absorbance difference spectrum in the 600–710 nm range at 77 K induced by continuous illumination (3 min of white light with approx. 50 mW/cm^2) of PS II core complexes from *Synechococcus* (40 μM Chl) when 3.3 mM ascorbate and 1.7 mM hydroquinone were added before freezing; $d = 0.36$ cm. Inset, the same in the 535–570 nm range. spectral resolution: 1 nm, scan speed: 50 nm/min, scan range: 710–520 nm.

of the Q_y band at 77 K. We obtain a yield of about 0.39 Car^+ and 0.47 Chl^+ per PS II reaction center. The decay of the long-lived states has been followed more precisely by measuring the recovery of the amplitude of the flash-induced absorbance change at 826 nm as function of the darktime after saturating illumination. A small fraction of about 15% recovers with half-lives ≤ 10 s; an additional 35% were found to be reversible in the time range of min with half-lives of about 2 min and 30 min. In the remaining 50% of the PS II reaction centers the states $Chl^+P680Q_A^-$ and $Car^+P680Q_A^-$ are stable ($t_{1/2} \geq 10$ h) at 77 K.

Fig. 6 shows the light-minus-dark absorbance difference spectrum measured in the presence of reduced Cyt *b*-559 after 5 min illumination. The C-550 bandshift associated with the reduction of Q_A and the absorbance decrease at 557 nm due to the oxidation of Cyt *b*-559 (see Fig. 6, inset) prove that it is the state Cyt b-$559^+Q_A^-$ which is formed preferentially under these conditions with a yield close to 100% using a differential extinction coefficient of 17500 M^{-1} cm^{-1} at 557 nm for the oxidation of Cyt *b*-559. In the wavelength region between 640 nm and 710 nm we observed band shifts of neighboring pigments (chlorophyll and/or pheophytin molecules) induced by the electric field of Cyt b-559^+ and Q_A^-, but the bleaching at 667 nm was strongly reduced (≤ 20% compared to that observed under oxidizing conditions). The band shifts are similar to those observed in the presence of oxidized Cyt *b*-559 (see Fig. 5, b,e). Again, the red shift of an absorption band giving rise to the absorbance decrease at 676 nm and the absorbance increase at 681 nm is most pronounced. The absorbance band in the near infrared around 1000 nm (not shown) was still observed, but the amplitude of the peak was reduced by a factor of ≥ 5 compared to that observed under oxidizing conditions. We assume that Cyt *b*-559 was not reduced in a small fraction of PS II reaction centers.

In order to clarify the pathways and kinetics of the electron transfer reactions in PS II at cryogenic temperatures, we have analyzed the decrease of the flash-induced absorbance change at 826 nm as function of the flash number, if the sample was excited by saturating flashes at a repetition rate of 4 Hz in the presence of oxidized Cyt *b*-559 (Fig. 7 trace a) and reduced Cyt *b*-559 (Fig. 7 trace b). The decrease of the amplitude results from the progressive accumulation of the long-lived (or stable) states with increasing flash number. Fig. 7 demonstrates that the accumulation occurs slightly faster and more efficiently in the presence of reduced Cyt *b*-559 (trace b). From the initial slope it follows that the amplitude decreases from flash to flash by about 5% (trace a) and 9% (trace b), respectively. Under the assumption that the electron donation from the secondary donor(s) to $P680^+$ occurs in competition to the charge recombination of $P680^+Q_A^-$, the amplitude of the flash-induced absorbance changes induced by the nth flash, ΔA_n, should decrease as

$$\Delta A_1 = \left(\frac{k_r}{k_r + k_s}\right)^{n-1}$$

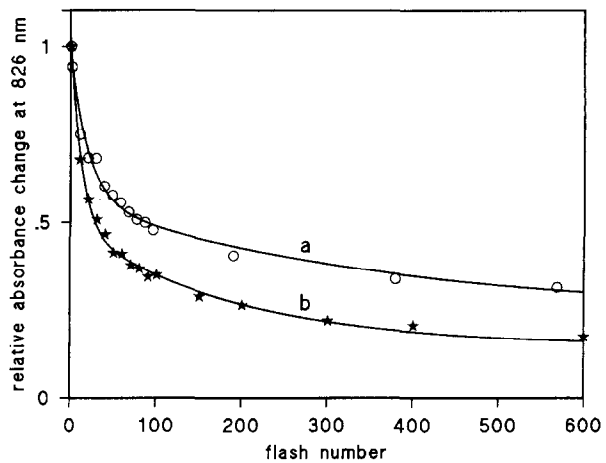

Fig. 7. Decrease of the flash-induced absorbance change at 826 nm as function of the flash number, if the sample was excited by saturating flashes at a repetition rate of 4 Hz in the presence of oxidized Cyt *b*-559 (trace a) and reduced Cyt *b*-559 (trace b). The decrease of the amplitude results from the progressive accumulation of the long-lived (or stable) states with increasing flash number. The curves in Fig. 9 are the best fit using the following fit function $\Delta A_n = p_1 \cdot \exp(-\ln(y_1 + 1)(n-1)) + p_2 \cdot \exp(-\ln(y_2 + 1)(n-1)) + p_3$ and the following parameters: trace a: $y_1 = 0.049$ (41.8%), $y_2 = 0.0027$ (34%) and const. = 24.2%; trace b: $y_1 = 0.081$ (50.7%), $y_2 = 0.0053$ (34.6%) and const. = 14.7%.

with k_r = rate constant for charge recombination of $P680^+Q_A^-$ and

$$k_s = \sum_{i=1}^{p} k_{si}$$

with p = number of secondary donors reducing $P680^+$ in parallel pathways and k_{si} = rate constant for electron donation from the secondary donor i. This equation can be written in the exponential form: $\Delta A_n = \Delta A_1 \cdot \exp(-\ln(y+1)(n-1))$ with $y = k_s/k_r$. The equation is, however, not sufficient to describe the experimental data as: (a) The amplitude does not drop to zero, but only to a minimum level of about 23% (trace a) and 13% (trace b). The remaining amplitude can be explained partly by the slow recombination of the oxidized secondary donor with Q_A in a fraction of the PS II reaction centers. Indeed, we observed that the size of the remaining amplitude is larger in the presence of oxidized Cyt *b*-559 and moreover, that it depends on the excitation rate. (b) The decrease of the amplitude was found to be not a single exponential but at least the sum of two exponentials. This suggests an inherent heterogeneity with respect to the rate constants k_r and k_{si} (see Discussion). The curves in Fig. 7 are the best fit using two exponential components plus a constant with the following parameters: trace a: $y_1 = 0.049$ (41.8%), $y_2 = 0.0027$ (34%) and const. = 24.2%; trace b: $y_1 = 0.081$ (50.7%), $y_2 = 0.0053$ (34.6%) and const. = 14.7%.

4. Discussion

In the present work, electron transfer reactions at 77 K in isolated PS II complexes from *Synechococcus* were studied by absorbance difference spectroscopy.

4.1. $P680^+Q_A^-/P680Q_A$ absorbance difference spectrum

A complete absorbance difference spectrum of $P680^+Q_A^-/P680Q_A$ measured with high spectral resolution at low temperature was not available until now. The difference spectrum (Fig. 3 and Fig. 4) exhibits the spectral features reported in earlier studies to be characteristic of secondary radical pair formation: the absorbance increase at 320 nm and the C-550 bandshift in the green wavelength region indicate the reduction of Q_A [45,23], whereas the spectrum in the near-infrared with the typical maximum around 820 nm [39] establishes the involvement of P680. Previously reported difference spectra at low temperature, which include the red wavelength region, were obtained with PS II subchloroplast fragments from spinach at 95 K [24] and with PS II particles from *Phormidium laminosum* at 100 K [25]. As discussed already by Reinman and Mathis [38], the results obtained with PS II subchloroplast fragments from spinach (especially the broad absorbance increase between 450 nm and 600 nm with a maximum at about 460 nm; the broad positive band at 760 nm and the decay with $t_{1/2} = 1.25$ ms) indicate contamination by chlorophyll *a* triplet formation. In both studies, the spectra exhibit a single bleaching band in the Q_y region centered at 680 nm similar to the $P680^+Q_A^-/P680Q_A$ spectrum at room temperature and they do not show the sharp features between 660 nm and 700 nm observed in this work (see Fig. 4). Possibly, the spectral resolution was too low in order to resolve the narrow bands.

As shown in Fig. 4, we found a strong temperature dependence of the $P680^+Q_A^-/P680Q_A$ spectrum in the Q_y region. At 77 K the maximum bleaching is at 675 nm, instead of 680 nm. The full width of the band at half maximum is only about 6 nm compared to about 15 nm of the 680 nm band at 295 K. The narrowing is accompanied by a corresponding increase of the peak amplitude.

The simplest way to explain the different positions of the maximum bleaching at 77 K and 295 K would be to assume that a blue shift of the P680 absorption band is induced upon lowering the temperature. However, a comparison with low temperature $^3P680/P680$ spectra rules out this possibility. The $^3P680/P680$ spectrum has been extensively studied using D1/D2/Cyt *b*-559-reaction center complexes from plants (for recent review see Refs: [29,30]) showing the bleaching maximum at 680.5 nm and a width of the main bleaching band of 5–8 nm. More recently, we examined the $^3P680/P680$ spectrum in the same preparation used in this work (O_2-evolving PS II core complexes from *Synechococcus*) and additionally in PS-II-enriched membrane fragments from spinach [42]. We found the maximum of the bleaching at 685 nm indicating that in more intact preparations the absorption band of P680 is located at 685 nm at low temperature (see also Ref. [46]). In contrast to these results, it is known from in vitro difference spectra of Chl a^+/Chl *a* and ^{3}Chl *a*/Chl *a* that the positions of the bleaching due to formation of the cation or the triplet state of Chl *a* are virtually identical, appearing at the maximum of the Q_y absorption band of Chl *a*. This leads to the question whether the positive charge and the triplet state are localized on the same pigment.

One possible explanation would be the migration of the triplet state formed by charge recombination of the primary radical pair from P680 to another chlorophyll absorbing at 685 nm. However, hole-burning experiments indicate that the triplet state is localized on P680 itself [47,48]. In addition, results from FTIR studies are consistent with the triplet state being located on P680 [49]. An alternative possibility, starting from the supposition that P680 absorbs at 685 nm at low temperature, would be an electron transfer from a chlorophyll with absorption maximum at 675 nm to $P680^+$. No evidence for such electron transfer was obtained from the kinetic analysis of the absorbance changes reported here. Furthermore, with the exception of the Q_y region, the 77 K difference spectrum closely

resembles that at 298 K attributed to $P680^+Q_A^-/P680Q_A$ (compare Fig. 3 with Fig. 3 of Ref. [10] and Fig. 4 inset with Fig. 6 of Ref. [39]). This indicates that the same species, P680 and Q_A, are monitored at both temperatures. Therefore, we prefer an interpretation of the different positions of the bleaching maxima found for the $P680^+Q_A^-/P680Q_A$ and $^3P680/P680$ spectra in which triplet and positive charge are assumed to be located on the same pigment with maximum absorption at 685 nm.

For an explanation, we propose that an electrochromic bandshift contributes strongly to the $P680^+Q_A^-/P680Q_A$ spectrum. The light-minus-dark absorbance difference spectra measured at 77 K in the presence of oxidized and reduced Cyt *b*-559 (Fig. 5 and Fig. 6) indicate that charge-separated states in PS II give rise to strong electrochromic band shifts in the Q_y region, i.e., the absorption bands of neighboring pigments (chlorophyll and/or pheophytin molecules) are shifted due to the electric field of the oxidized donor and Q_A^-. The predominant feature is the red shift of an absorption band giving rise to the absorbance decrease at 676 nm and the absorbance increase at 681 nm (Fig. 5 and Fig. 6). Further evidence for this proposal comes from the temperature dependence of the $P680^+Q_A^-/P680Q_A$ spectrum presented elsewhere [42]. The temperature dependence indicates that an electrochromic band shift increases strongly upon lowering the temperature. This can be explained for the most part by the narrowing of absorption bands at low temperature.

A possible explanation of the 77 K $P680^+Q_A^-/P680Q_A$ spectrum describing the main features quite well can be achieved using the following assumptions: (a) The formation of $P680^+$ leads to a bleaching at 685 nm. (b) The electrochromic red shift of an absorption band located at about 675 nm gives rise to the absorbance decrease at 675 nm and the absorbance increase at 683 nm. The absorbance increase partly cancels out the bleaching at 685 nm resulting in a positive band at 681 nm. The assumption of an electrochromic shift of several nanometers is not unreasonable according to calculations for the electrochromic effect on the BChl monomer due to a charge on the special BChl pair in the bacterial reaction center [50]. Additionally, a smaller electrochromic shift of an absorption band centered at about 685 nm due to the electric field of Q_A^- [23] might contribute to the spectral features observed at 681 and 686 nm (Fig. 4). At room temperature this bandshift (positive peak at 680 nm, negative peak at 690 nm) is probably also superimposed on the bleaching of P680, giving rise to the asymmetric broadening of the bleaching band on the long wavelength side with the zero crossing at 700 nm (see Fig. 4). Indeed, the room-temperature spectrum of $P680^+Tyr_Z/P680Tyr_Z^+$ is more symmetrical and has the zero crossing at 694 nm [41]. (c) The absorbance increase at 665 nm may be attributed to the appearance of an absorption band from the Chl *a* cation radical [20–22] located at this wavelength, because pigment–protein interactions are changed by the formation of the Chl *a* cation. Fig. 8, top, illustrates the deconvolution of the measured $P680^+Q_A^-/P680Q_A$ spectrum using the components described above. The bottom of the figure shows that the calculated difference spectrum (= sum of the components depicted in Fig. 8, top) resembles closely the 77 K $P680^+Q_A^-/P680Q_A$ difference spectrum taken from Fig. 4.

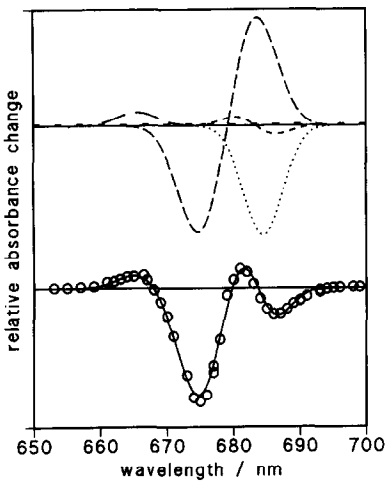

Fig. 8. Top: Deconvolution of the $P680^+Q_A^-/P680Q_A$ difference spectrum measured at $T = 77$ K. The oxidation of P680 leads to the bleaching of a Gaussian band centered at 684.5 nm, fwhm = 7 nm and relative amplitude of −1. The formation of the cation is taken into account as an absorbance increase of a band centered at 665.5 nm, fwhm = 7 nm and relative amplitude of 0.125 and a constant of 0.015. Contributions of electrochromic bandshifts are taken into account as follows: two Gaussian bands (relative amplitudes of −1 and −0.31, fwhm of 7.5 and 7 nm) are shifted from 674.9 nm to 683.5 nm and from 684 nm to 682.7 nm. Bottom: Comparison between the calculated $P680^+Q_A^-/P680Q_A$ difference spectrum (= sum of the components depicted in the upper part) (solid line) with the measured $P680^+Q_A^-/P680Q_A$ spectrum taken from Fig 4.

The simulation described above shows that the spectral features of P680 are well described using the assumption that P680 is essentially a monomeric chlorophyll that is only weakly coupled to its neighboring pigments. The small spectral features due to the loss of weak excitonic coupling as observed in the $^3P680/P680$ spectrum [42,46,48] have been neglected for the sake of simplicity. The conclusion that P680 can be considered at first approximation as a monomeric chlorophyll is supported by other properties of P680 (e.g., the small Stark effect, the high redox potential, the zero-field splitting parameters of P680 triplet (for reviews see Refs. [29,30,32,33]).

4.2. Kinetics of charge recombination between $P680^+$ and Q_A^-

In PS II core complexes from *Synechococcus*, the charge recombination between $P680^+$ and Q_A^- was found to deviate from a single exponential process. At low temperatures the time-course of charge recombination could be deconvoluted into two components with half-lives of (1.8 ± 0.4)

ms and (5.0 ± 1.0) ms (see Fig. 2). The difference spectra of both components exhibit the spectral features characteristic of $P680^+Q_A^-$ recombination at low temperature. Therefore it can be ruled out that Chl triplet is the origin of the faster phase. Measurements with higher spectral resolution are in preparation to look for spectral differences between both components near the isosbestic points similar to those reported for bacterial reaction centers [13–15]. At room temperature the deviations from a single exponential decay are even more pronounced. In accordance with our previous report [10] the decay of the flash-induced absorbance changes could be described by three exponential phases with half-lives of about 180 μs, 800 μs and 6 ms. Virtually identical spectra of the three phases between 250 nm and 550 nm show that all three phases arise from the charge recombination between $P680^+$ and Q_A^- [10]. The recombination rate is essentially temperature-independent below 200 K, indicating that the recombination proceeds via a tunneling process. Above ≈ 200 K, the rate increases with increasing temperature, i.e., the recombination occurs predominantly by a thermally activated process.

A similar behavior has been reported for the recombination kinetics of the secondary radical pair in reaction centers from *Rhodopseudomonas viridis* [14,15]. The kinetics are biphasic at room temperature and become closer to mono-exponential at low temperature. The recombination rate is essentially temperature-independent at low temperature. Above ≈ 240 K the temperature dependence indicates an activated process which has been proposed to proceed through a thermally populated intermediate state that could be a relaxed form of the primary radical pair [14]. In native reaction centers from *Rhodobacter sphaeroides*, on the other hand, non-exponential recombination kinetics were also observed at low temperature but exponential kinetics at room temperature [12]. The rate is almost temperature-independent, actually becoming somewhat faster with decreasing temperature, indicating that the thermally activated reaction pathway does not contribute to the recombination of the secondary radical pair.

The low-temperature biphasicity of the recombination kinetics observed in bacterial reaction centers has been assigned to two (or a distribution of) slightly different conformational states trapped at low temperature [12–15]. Thereby it was assumed that the distance between donor and acceptor varies between different conformations of the protein. Due to the exponential dependence of the electron transfer rate on the donor–acceptor distance, rather small changes could explain the observed half-lives of the two phases differing by a factor of about 3. The biphasicity of the $P680^+Q_A^-$ recombination kinetics observed in this work in PS II complexes at low temperature has presumably the same origin. As the kinetics of the recombination process become rather close to mono-exponential at low temperature, the reaction centers may freeze preferentially into an energetically most favorable conformational state.

The strong non-exponential behavior of $P680^+Q_A^-$ recombination kinetics observed in PS II complexes at room temperature appears to be related to the observed activated temperature dependence of the electron transfer rate. Therefore, we assume that a distribution of activation enthalpies gives rise to the non-exponential recombination kinetics at room temperature. The different activation enthalpies might be due to heterogeneities of the PS II complexes. EPR measurements indicate for example that two forms of $Q_A^-Fe^{2+}$ are present in PS II preparations with different iron–semiquinone interactions [51]. Furthermore, different states of the second quinone acceptor (Q_B or Q_B^-) might influence the free energy level of $P680^+Q_A^-$. Different structural states of the reaction center protein could also explain the non-exponential kinetics at room temperature. However, at room temperature the protein fluctuates between these states and a non-exponential time-course results only when the characteristic time constant of these fluctuations is large compared to the time constant of charge recombination.

4.3. Scheme of electron transfer reactions at 77 K

After the flash-induced formation of $P680^+$ Q_A^-, $P680^+$ decays almost completely by charge recombination. With low yield (< 10%) $P680^+$ is reduced by competitive electron donation from secondary donors. In agreement with earlier work in the literature performed with PS II preparations of higher plants [6–9] we identified three secondary donors functioning in PS II of *Synechococcus*: Cyt *b*-559 characterized by the absorbance decrease at 557 nm, a carotenoid characterized by the absorbance increase around 1000 nm and a chlorophyll *a* characterized by the bleaching at 667 nm. When the Chl was first identified to be a secondary donor to $P680^+$ at low temperature it was characterized by a bleaching near 676 nm [7]. Fig. 5 and Fig. 6 show, however, that the negative band at 676 nm is most probably due to an electrochromic shift in the Q_y transition energy of a Chl, as is manifested by a first-derivative-type absorbance change spectrum around 680 nm. The about 10 G wide EPR signal observed near $g = 2.0$ in the presence of oxidized Cyt *b*-559 at low temperature has been attributed initially to an oxidized chlorophyll [7]. Fig. 5 shows that both Chl and Car cation radicals are present under these conditions and both may contribute to the characteristic EPR signal (see also Ref. [52]). Photooxidation of a carotenoid and a chlorophyll which absorbs near 667 nm has been reported to occur also at room temperature in D1/D2/Cyt *b*-559-reaction center complexes in the presence of silicomolybdate [53,54]. It has been proposed that the photooxidation of these chromophores of the reaction center might be the initial step of photoinhibition on the donor side of PS II induced by strong light at room temperature.

In the following, we discuss the pathways for electron donation to $P680^+$ at low temperature. If Cyt *b*-559 is

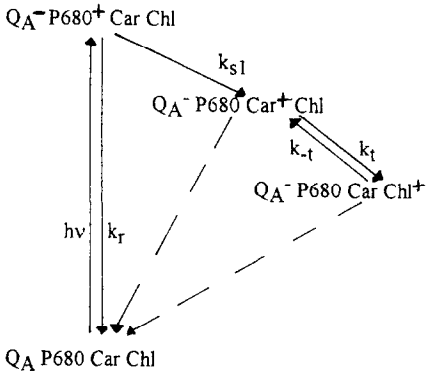

Scheme 1.

chemically oxidized, the reaction scheme must account for the following observations: (1) Both carotenoid and chlorophyll are photooxidized at a ratio of about 1:1 (see Results). It should be noted that this ratio can only be a rough estimation due to the uncertainty of the differential extinction coefficients of Car^+/Car and Chl^+/Chl. (2) After single flash excitation, $P680^+$ is reduced in $\leq 5\%$ of the reaction centers by a secondary donor, otherwise by charge recombination. (3) The rise of Car^+ formation after a single turnover flash is significantly faster than the charge recombination of $P680^+Q_A^-$ ($t_{1/2} = 1.9$ ms in *Synechococcus*, not shown; see also Ref. [8]). (4) A slow recombination of the oxidized secondary donor with Q_A^- occurs in about half the reaction centers.

If one assumes that Car and Chl donate electrons to $P680^+$ by parallel pathways, both donors should be oxidized at the same rate with which $P680^+$ becomes reduced. This is in contradiction to (3) and therefore, we prefer a kinetic scheme with one sequential pathway (Scheme 1). This scheme offers an explanation for the more complex kinetic behavior. If the equilibrium between the two states, $Q_A^-P680Car^+Chl$ and $Q_A^-P680CarChl^+$, is achieved sufficiently fast, the rise of Car^+ formation becomes apparently faster than the decay of $Q_A^-P680^+$. Fig. 9 shows the time-course of the populations of the states $Q_A^-P680^+CarChl$ (squares), $Q_A^-P680Car^+Chl$ (triangles)

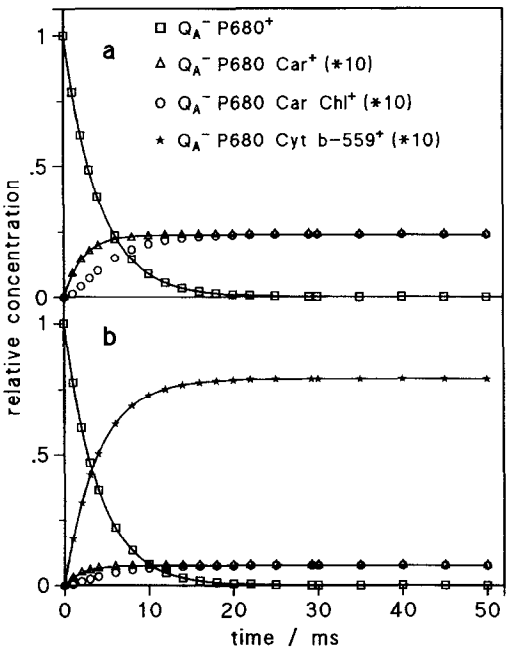

Fig. 9. (a) Relative concentration of the radical pairs calculated according to Scheme 1 with rate constants: $k_r = 230\ s^{-1}$, $k_{s1} = 11.55\ s^{-1}$, $k_t = k_{-t} = 300\ s^{-1}$. (b) Relative concentration of the radical pairs calculated according to Scheme 2 with constants: $k_r = 230$, $k_{s1} = 3.8\ s^{-1}$, $k_{s2} = 20\ s^{-1}$, $k_t = k_{-t} = 300\ s^{-1}$. Note that the amplitudes of all radical pairs involving secondary donors are enlarged by a factor of 10. For further details see text.

and $Q_A^-P680CarChl^+$ (circles) calculated with the rate constants given in the figure legend. The solid lines represent exponentials with half-lives of 3 ms and 1.7 ms for the decay of $P680^+$ and the formation of Car^+ respectively in accordance with the experimental results.

It should be noted that the model does not account for (a) the biphasicity of the $P680^+$ decay (Fig. 2) and (b) the multiphasic accumulation of the states $Q_A^-P680Car^+Chl$ and $Q_A^-P680CarChl^+$ with increasing flash number (Fig. 7, trace a). These observations reflect presumably an inherent heterogeneity of the rate constants. A pronounced heterogeneity was also observed for the slow decay of the

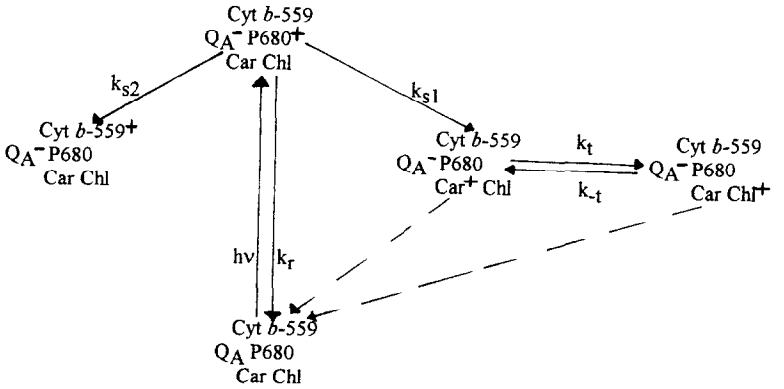

Scheme 2.

states Q_A^-P680Car$^+$Chl and Q_A^-P680CarChl$^+$. The dashed arrows in Scheme 1 indicate that these states decay by only approximately 50%.

If Cyt *b*-559 is reduced, the extension of Scheme 1 must account for the following observations. (1) Continuous illumination leads to the preferential oxidation of Cyt *b*-559. (2) After single flash excitation, P680$^+$ is reduced in $\leq 10\%$ of the reaction centers by a secondary donor, otherwise by charge recombination. (3) The rate of Cyt *b*-559$^+$ formation after a single turnover flash is similar to that of charge recombination between P680$^+$ and Q_A^- (not shown, see also Ref. [3,4]). (4) The amplitude of the flash-induced absorbance change at 980 nm attributable to carotenoid cations is several-fold smaller compared to that observed in the presence of oxidized Cyt *b*-559 [8]. (5) The state Q_A^-P680CarChlCyt *b*-559$^+$ is stable at 77 K.

It is a subject of controversy whether Cyt *b*-559 reduces P680$^+$ directly or via another component [4,7,9]. According to our results we consider it to be more likely that Cyt *b*-559 reduces P680$^+$ directly (see Scheme 2). This is supported by the observation that Cyt *b*-559 becomes oxidized at the same rate with which P680$^+$ becomes reduced. The assumption, that Cyt *b*-559 and Car donate electrons to P680$^+$ in parallel pathways, explains in a simple way why the accumulation of long-lived states occurs faster with increasing flash number in the presence of reduced Cyt *b*-559 (see Fig. 7).

Since P680$^+$ decays for the most part ($\geq 90\%$) by charge recombination with rate constant k_r, it follows $k_r \gg k_{s1}$ and k_{s2}. In this case, Scheme 2 predicts that the yield, ϕ, of Car$^+$ should be approximately the same in the presence of oxidized ($\phi = k_{s1}/(k_r + k_{s1})$) or reduced Cyt *b*-559 ($\phi = k_{s1}/(k_r + k_{s1} + k_{s2})$). We observed, however, that the amplitude of the flash-induced absorbance change at 980 nm attributable to carotenoid cations is smaller by a factor of about 3 in the presence of reduced Cyt *b*-559 (not shown). This indicates a lower value of k_{s1} when Cyt *b*-559 is reduced. The standard free energy change for the reaction P680$^+$Car $\rightarrow$ P680Car$^+$ might be influenced by the redox state of the Cyt *b*-559 due to electrostatic interactions of the positively charged oxidized Cyt *b*-559 with P680$^+$ and Car$^+$. According to the dependence of the electron transfer rate on the free energy of the reaction, this could explain different values of k_{s1} in the presence of reduced or oxidized Cyt *b*-559. Fig. 9b shows the time-course of the populations of the states Q_A^-P680$^+$ (squares), Q_A^-P680Car$^+$ (triangles), Q_A^-P680CarChl$^+$ (circles) and Q_A^-P680Cyt *b*-559$^+$ (stars) calculated with the rate constants given in the figure legend. The solid lines represent exponentials with a half-life of 3 ms for the decay of P680$^+$ and the formation of Cyt *b*-559$^+$ and of 1.7 ms for the rise of Car$^+$ formed with a 3-fold lower yield in accordance with the experimental results.

The proposal that Cyt *b*-559 is a direct electron donor to P680$^+$ is in contradiction to conclusions drawn from EPR measurements. Thompson and Brudvig [9] determined the intensities of EPR signals attributed to the S_2 state of the Mn-complex, oxidized Cyt *b*-559 and oxidized Chl as function of temperature. Our data suggest that the EPR signal around $g = 2$ attributed to Chl$^+$ by these authors arises presumably from both the Chl and the Car cation radical (see also Ref. [52]). They found that the yield of Cyt *b*-559$^+$ under reducing conditions and the yield of Chl$^+$ under oxidizing conditions are decreasing in parallel with the increase of the yield of the S_2 state. They concluded that this observation, together with the preferential photooxidation of Cyt *b*-559 under reducing conditions, is only consistent with a sequential electron donation pathway, i.e., Chl is the direct donor to P680$^+$ and is in turn rereduced by Cyt *b*-559. A problem of this conclusion is that the temperature dependence of the rate constants for the reduction of P680$^+$ by the Mn-complex, Cyt *b*-559, Car and Chl are not known. The observed temperature dependence of the yields is probably dominated by the strong temperature dependence of the formation of the S_2 state. Furthermore, as discussed above, this result can also be explained using the model of parallel pathways (Scheme 2) assuming that the rate constant for the oxidation of the donor giving rise to the $g = 2$ signal is influenced by the redox state of Cyt *b*-559 due to electrostatic interactions.

In summary, the kinetic data presented in this work and those published earlier [3,4,8,9] can be explained best using a model with Cyt *b*-559 and Car donating electrons directly to P680$^+$ in parallel pathways. The Car$^+$ is subsequently rereduced by Chl down to an equilibrium level.

Acknowledgements

We wish to thank Ms. Dörte DiFiore and Ms. Claudia Otto for preparing the PS II complexes and Dr Fraser MacMillan for critical reading of the manuscript. This work was supported by grants from the Deutsche Forschungsgemeinschaft (Sonderforschungsbereich 312, Teilprojekt A5).

References

[1] Mathis, P. and Rutherford, A.W. (1987) in New Comprehensive Biochemistry: Photosynthesis (Amesz, J., ed.), pp. 63–96, Elsevier, Amsterdam.
[2] Hansson, Ö. and Wydrzynski, T. (1990) Photosynth. Res. 23, 131–162.
[3] Floyd, R.A., Chance, B. and Devault, D. (1971) Biochim. Biophys. Acta 226, 103–112.
[4] Mathis, P. and Vermeglio, A. (1975) Biochim. Biophys. Acta 396, 371–381.
[5] Malkin, R. and Bearden, A.J. (1975) Biochim. Biophys. Acta 396, 250–259.
[6] Vermeglio, A. and Mathis, P. (1973) Biochim. Biophys. Acta 292, 763–771.
[7] Visser, J.W.M., Rijgersberg, C.P. and Gast, P. (1977) Biochim. Biophys. Acta 460, 36–46.

[8] Schenck, C.C., Diner, B., Mathis, P. and Satoh, K. (1982) Biochim. Biophys. Acta 680, 216–227.
[9] Thompson, L.K. and Brudvig, G.W. (1988) Biochemistry 27, 6653–6658.
[10] Gerken, S., Dekker, J.P., Schlodder, E. and Witt, H.T. (1989) Biochim. Biophys. Acta 977, 52–61.
[11] Gerken, S. (1989) Doctoral Thesis, Technische Universität Berlin.
[12] Feher, G., Okamura, D. and Kleinfeld, D. (1987) in Protein Structure (Austin, R., Buhks, E., Chance, B., DeVault, D. Dutton, P.L., Frauenfelder, H. and Gol'danskii, V.I., eds.), pp. 399–422, Springer, Berlin.
[13] Parot, P., Thiery, J. and Vermeglio, A. (1987) Biochim. Biophys. Acta 893, 534–543.
[14] Sebban, P. and Wraight, C.A. (1989) Biochim. Biochim. Acta 974, 54–65.
[15] Baciou, L., Rivas, E. and Sebban, P. (1990) Biochemistry 29, 2966–2976.
[16] Frauenfelder, H., Parak, F. and Young, R.D. (1988) Ann. Rev. Biophys. Biophys. Chem. 17, 451–479.
[17] Dekker, J.P., Boekema, E.J., Witt, H.T. and Rögner, M. (1988) Biochim. Biophys. Acta 936, 307–318.
[18] Döring, G., Stiehl, H.H. and Witt, H.T. (1967) Z. Naturforsch. 22b, 639–644.
[19] Van Gorkom, H.J., Pulles, M.P.J. and Wessels, J.S.C. (1975) Biochim. Biophys. Acta 408, 331–339.
[20] Borg, D.C., Fajer, J., Felton, R.H. and Dolphin, D. (1970) Proc. Natl. Acad. Sci. USA 67, 813–820.
[21] Davis, M.S., Forman, A. and Fajer, J. (1979) Proc. Natl. Acad. Sci. USA 76, 4170–4174.
[22] Chauvet, J.-P., Viovy, R., Santus, R. and Land, E.J. (1981) J. Phys. Chem. 85, 3449–3456.
[23] Van Gorkom, H.J. (1974) Biochim. Biophys. Acta 347, 439–442.
[24] Ke, B. and Dolan, E. (1980) Biochim. Biophys. Acta 590, 401–406.
[25] Ke, B., Inoue, H., Babcock, G.T., Fang, Z.-X. and Dolan, E. (1982) Biochim. Biophys. Acta 682, 297–306.
[26] Den Blanken, H.J., Hoff, A.J., Jongenelis, A.P.J.M. and Diner, B. (1983) FEBS. Lett. 157, 21–26.
[27] Takahashi, Y., Hansson, Ö., Mathis, P. and Satoh, K. (1987) Biochim. Biophys. Acta 893, 49–59.
[28] Durrant, J.R., Giorgi, L.B., Barber, J., Klug, D.R. and Porter, G. (1990) Biochim. Biophys. Acta 1017, 167–175.
[29] Seibert, M. (1993) in The Photosyntetic Reaction Center (Deisenhofer, J. and Norris, J.R., eds.), Vol. I, pp. 319–356, Academic Press, San Diego.
[30] Van Grondelle, R., Dekker, J.P., Gillbro, T. and Sundstrom, V. (1994) Biochim. Biophys. Acta 1187, 1–65.
[31] Michel, H. and Deisenhofer, J. (1988) Biochemistry 27, 1–7.
[32] Rutherford, A.W. (1986) Biochem. Soc. Trans. 14, 15–17.
[33] Van Gorkom, H.J. and Schelvis, J.P.M. (1993) Photosynth. Res. 38, 297–301.
[34] Schatz, G.H. and Witt, H.T. (1984) Photobiochem. Photobiophys. 7, 1–14.
[35] Rögner, M., Dekker, J.P., Boekema, E.J. and Witt, H.T. (1987) FEBS. Lett. 219, 207–211.
[36] Schlodder, E. and Meyer, B. (1987) Biochim. Biophys. Acta 890, 23–31.
[37] Haveman, J., Mathis, P. and Vermeglio, A. (1975) FEBS. Lett. 58, 259–261.
[38] Reinman, S. and Mathis, P. (1981) Biochim. Biophys. Acta 635, 249–258.
[39] Mathis, P. and Setif, P. (1981) Isr. J. Chem. 21, 316–320.
[40] Shipman, L.L., Cotton, T.M., Norris, J.R. and Katz, J.J. (1976) J. Am. Chem. Soc. 98, 8222–8230.
[41] Schlodder, E., Brettel, K., Schatz, G.H. and Witt, H.T. (1984) Biochim. Biophys. Acta 765, 178–185.
[42] Hillmann, B., Brettel, K. Van Mieghem, F.J.E., Kamlowski, A., Rutherford, A.W. and Schlodder, E. (1995) Biochemistry 34, 4814–4827.
[43] De Paula, J.C., Innes, J.B. and Brudvig, G.W. (1985) Biochemistry 24, 8114–8120.
[44] Chauvet, J.P., Viovy, R., Land, E.J., Santus, R. and Truscott, T.G. (1983) J. Phys. Chem. 87, 592–601.
[45] Stiehl, H.H. and Witt, H.T. (1968) Z. Naturforsch. 23b, 220–224
[46] Carbonera, D., Giacometti, G. and Agostini, G. (1994) FEBS Lett. 343, 200–204.
[47] Jankowiak, R. and Small, G.J. (1993) in Photosynthetic Reaction Centers (Deisenhofer, J. and Norris, J., eds.), Vol. II, pp. 133–177, Academic Press, San Diego.
[48] Kwa, S.L.S., Eijckelhoff, C., Van Grondelle, R. and Dekker, J.P. (1994) J. Phys. Chem. 98, 7702–7711.
[49] Noguchi, T., Inoue, Y. and Satoh, K. (1993) Biochemistry 32, 7186–7195.
[50] Eccles, J., Honig, B. and Schulten, K. (1988) Biophys. J. 53, 137–144.
[51] Zimmermann, J.L. and Rutherford, A.W. (1986) Biochim. Biophys. Acta 851, 416–423.
[52] Blubaugh, D.J., Atamian, M., Babcock, G.T., Goldbeck, J.H. and Cheniae, G.M. (1991) Biochemistry 30, 7586–7597.
[53] Telfer, A., De Las Rivas, J. and Barber, J. (1991) Biochim. Biophys. Acta 1060, 106–114.
[54] Takahashi, Y., Satoh, K. and Itoh, S. (1989) FEBS Lett. 255, 133–138.